JCI The Journal of Clinical Investigation

Eltrombopag inhibits TET dioxygenase to contribute to hematopoietic stem cell expansion in aplastic anemia

Yihong Guan, Metis Hasipek, Dongxu Jiang, Anand D. Tiwari, Dale R. Grabowski, Simona Pagliuca, Sunisa Kongkiatkamon, Bhumika Patel, Salendra Singh, Yvonne Parker, Thomas LaFramboise, Daniel Lindner, Mikkael A. Sekeres, Omar Y. Mian, Yogen Saunthararajah, Jaroslaw P. Maciejewski, Babal K. Jha

J Clin Invest. 2022. https://doi.org/10.1172/JCI149856.

Research In-Press Preview Hematology

Graphical abstract

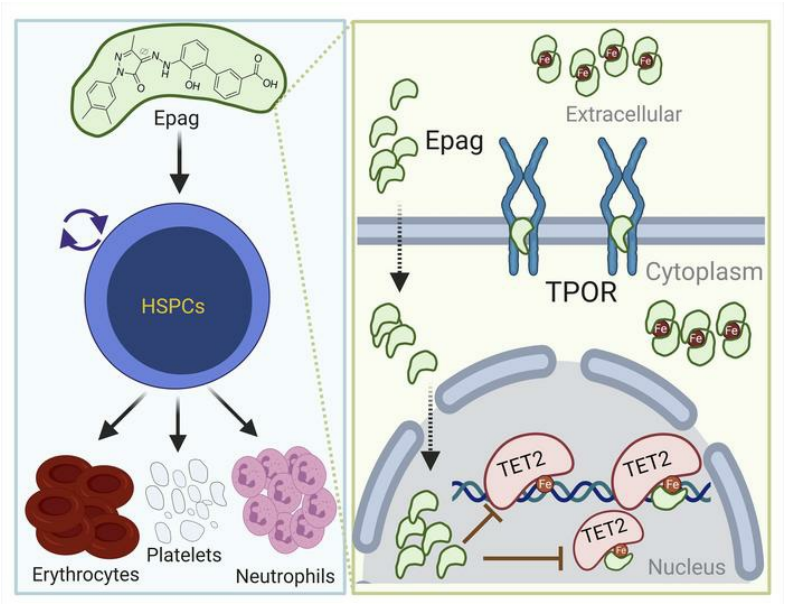

Eltrombopag inhibits TET Dioxygenase to Contribute to Hematopoietic Stem Cell Expansion in Aplastic Anemia

Yihong Guan[1], Metis Hasipek[1], Dongxu Jiang[1], Anand D. Tiwari[1], Dale R. Grabowski[1], Simona Pagliuca[1], Sunisa Kongkiatkamon[1], Bhumika Patel[2], Salendra Singh[3], Yvonne Parker[1], Thomas LaFramboise[3], Daniel Lindner[1,4,5], Mikkael A. Sekeres[2,6], Omar Y. Mian[1,4,5], Yogen Saunthararajah[1,2,4,5], Jaroslaw P. Maciejewski[1,2,4,5]*, and Babal K. Jha[1,4,5]*

[1]Department of Translational Hematology and Oncology Research, [2]Leukemia Program, Department of Hematologic Oncology and Blood Disorders, Taussig Cancer Institute, Cleveland Clinic, [3]Department of Genetics and Genome Sciences, School of Medicine, Case Western Reserve University, [4]Cleveland Clinic Lerner College of Medicine, Cleveland Clinic [5]Developmental Therapeutics, Case Comprehensive Cancer Center, Cleveland, OH 44106, USA.

[6]Current affiliation: Sylvester Comprehensive Cancer Center, Department of Biochemistry and Molecular Biology, University of Miami Miller School of Medicine, Miami, FL; USA.

*__Corresponding Authors:__

1) Babal K. Jha, 9500 Euclid Avenue, NE6, Cleveland, OH 44195, 216-444-6739, jhab@ccf.org.

2) Jarosław P. Maciejewski, 9500 Euclid Avenue, NE6, Cleveland, OH 44195, 216-445-5962, maciejj@ccf.org

Running Title: Eltrombopag Directly Inhibits TET2

Keywords: Eltrombopag, TET2, stem cells, aplastic anemia

Key Points

- Eltrombopag directly binds to the TET2 catalytic domain and inhibits its dioxygenase activity mimicking loss of TET2 functions in vitro and in vivo.
- Eltrombopag treatment restricts clonal evolution of TET2 mutant myeloid cells

Abstract

Eltrombopag, an FDA-approved non-peptidyl thrombopoietin receptor agonist is clinically used for the treatment of aplastic anemia, a disease characterized by hematopoietic stem cell failure and pancytopenia, to improve platelet counts and stem cell function. Eltrombopag treatment results in a durable tri-lineage hematopoietic expansion in patients. Some of the eltrombopag hematopoietic activity has been attributed to its off-target effects including iron chelation properties. However, the mechanism of action for its full spectrum of clinical effects is still poorly understood. Here, we report that eltrombopag bound to the TET2 catalytic domain and inhibited its dioxygenase activity, which was independent of its role as an iron chelator. The DNA demethylating enzyme TET2, essential for hematopoietic stem cell differentiation and lineage commitment, is frequently mutated in myeloid malignancies. Eltrombopag treatment expanded TET2 proficient normal hematopoietic stem and progenitor cells, in part, due to its ability to mimic loss of TET2 with simultaneous thrombopoietin receptor activation. On the contrary, TET inhibition in TET2 mutant malignant myeloid cells prevented neoplastic clonal evolution, in vitro and in vivo. This mechanism of action may offer a restorative therapeutic index and provide a scientific rationale to treat selected patients with TET2-mutant or TET-deficiency-associated myeloid malignancies.

Introduction

Idiopathic aplastic anemia (AA) is characterized by immune-mediated hematopoietic progenitor and stem cells (HSPCs) destruction resulting in deficiencies across all hematopoietic lineages (1-3). Despite the therapeutic successes of immunosuppressive therapies (IST), approximately one-third of patients remain refractory (4) and many of the responses are incomplete. Moreover, some AA patients may experience clonal progression to myelodysplastic syndrome (MDS), associated with a poor prognosis (5-9). Recently, a synthetic thrombopoietin receptor (TPOR) agonist, eltrombopag (Epag) has been shown to be effective in AA (10). In addition to the anticipated effect on platelet counts, Epag therapy also produced remarkable tri-lineage hematopoiesis (6, 11, 12). Subsequent studies confirmed the efficacy of Epag in de novo as well as in refractory AA (13) increasing both the magnitude of response and the number of responders. These effects expanded the indication spectrum of Epag from immune thrombocytopenic purpura to AA, establishing this drug as an essential hematologic therapeutic.

TPOR expressed on megakaryocytes typically signals via JAK/STAT pathway activation, but the presence of this receptor on early HSPCs could contribute to its stimulatory effects driving the production of other blood cell lineages. However, Epag's hematopoietic activity has been observed in murine models despite its inability to bind or activate murine TpoR. A similar finding has also been confirmed in TpoR-deficient mice (14-17) in which Epag treatment remarkably expanded HSPCs. These observations suggested that some of Epag's activities may be TPOR independent, in contrast to peptide TPO analogs, e.g., romiplostim. These TPOR independent effects of Epag were hypothesized to be due to its iron (III) chelating properties (14, 16, 17), but the molecular mechanism as to how this iron (III)-binding could drive the HSPCs expansion remains speculative.

Epag effects on intracellular iron may affect certain iron-dependent epigenetic pathway/s that promote HSPCs self-replication. For instance, TET-dioxygenases (TET1-3) are Fe^{2+}- and α-

ketoglutarate-(αKG)-dependent DNA dioxygenases, which mediate CpG demethylation of promoters and enhancers in HSPCs. Consequently, by changing gene expression patterns, TETs control HSPC expansion and differentiation (18, 19). TET2 is the most abundant TET-dioxygenase in HSPCs, and somatic loss-of-function (LOF) mutations of this gene frequently occur in myeloid neoplasia and clonal hematopoiesis of indeterminate potential (CHIP), a prodromal condition in otherwise healthy elderly individuals associated with a higher rate of progression to leukemia compared to non-CHIP patients (20).

Here we report the results of experiments designed to determine whether Epag affects the function of TET-dioxygenases. Our findings clarify the mode of action of this drug in the HSPC compartment, specifically Epag's activity in promoting multi-lineage clonal expansion and thus its therapeutic efficacy in AA.

RESULTS

The mechanisms of Epag action. Clinical and experimental observations suggest that a significant part of the hematopoietic activities of Epag is independent of its ability to activate TPOR mediated signaling (14). During the search for TET-dioxygenase modulators performed using an in-house developed cell-free high-throughput screen employing a bioactive small molecule library (LOPAC1280 and Selleck's L1700; Figure 1A and Supplemental Figure 1A), Epag emerged as one of the most potent inhibitors of TET-dioxygenase activity targeting the TET2 catalytic domain ($TET2^{CD}$). The IC50 for TET1 (1.0 ±0.1μM), TET2 (1.3±0.3μM), and TET3 (1.8 ±0.1μM) dioxygenases calculated from the dose-response curves suggest that Epag inhibits all 3 TET-dioxygenases with a similar efficacy even in the presence of 25-fold molar excess of Fe^{2+} (Figure 1B). To test whether Epag is a competitive inhibitor of TET co-factors we performed dose-dependent TET-dioxygenase inhibition in the presence of 25 and 250μM of αKG or Fe^{2+}. The IC50 of Epag under excess of Fe^{2+} or αKG remained unaffected (Figure 1C). The results indicate that Epag does not compete at the αKG binding site, since 10-fold molar excesses do not affect

its ability to inhibit TET2-dioxygenase. The hematopoietic activity of Epag has been attributed to cellular and extracellular Fe^{3+} chelation (14, 17, 21, 22). Therefore, to probe the effect of free iron sequestration by Epag on its ability to inhibit TET-activity, we pre-incubated excess Epag (25μM) with varying concentrations of Fe^{2+} or Fe^{3+} and performed TET-dioxygenase activity assays. The addition of up to 8-fold molar excess of either form of iron (Fe^{2+} or Fe^{3+}) did not rescue TET enzymatic activity (Supplemental Figure 1B). However, the addition of 75 μM of Fe^{3+} changed the IC50 of Epag from 1.3 μM to 5.1 μM (Figure 1D). This shift in the IC50 of Epag on TET inhibition was consistent with the proposed model of Epag sequestering free Fe^{3+}. However, TET-dioxygenase inhibition by Epag is not fully attributable to its affinity for Fe^{3+} as 100-fold molar excess of Fe^{3+} did not reverse TET dioxygenase inhibition. In addition, to test if iron chelators can act as broad-spectrum inhibitors of TET-dioxygenase activity, we tested deferoxamine (DFO) in similar conditions and found that iron chelation does not inhibit TET-dioxygenase activity (Figure 1E). These results suggest Epag's effects on TET2 are independent of its ability to chelate Fe^{3+}.

To further elucidate the specificity of Epag-mediated TET2 inhibition, we performed surface plasmon resonance-based analysis to measure the direct binding to $TET2^{CD}$ (Figure 1F). We observed a dose-dependent increase in the resonance response consistent with the direct binding of Epag to immobilized TET2 on a sensor chip (Figure 1G). However, we did not observe any significant affinity of Epag for TET2 in the absence of Fe^{2+}. The addition of Fe^{3+} in place of Fe^{2+} significantly reduced the binding of Epag to TET2. DFO, a known broad-spectrum iron chelator, did not show $TET2^{CD}$ binding or inhibitory activity (Figure 1G). This result further confirmed the notion that TET inhibition by Epag is not due to free iron chelation. To further understand the mode of binding of Epag to TET2 we performed in silico docking (Autodock 4) running on auto dock tools (23) with the known crystal structure of $TET2^{CD}$ (PDB ID: 4NM6) and interaction with its cofactors and substrates (24). Docking results indicated that Epag can form a tripartite complex with Fe^{2+} and TET2 (Figure 1H and Supplemental Figure 1D). The predictive model accounting for our binding data suggests a probable mode of Epag interaction with TET2 that incorporates

His1382, Asp1387, and His1904 residues, while also engaging the catalytic site Fe^{2+} (Supplemental Figure 1C-D). These amino acids are conserved among the family of TET dioxygenases, TET1 and TET3, and in their murine homologs (Supplemental Figure 1E).

Epag diffuses into the nucleus*.* There have been several reports characterizing Epag's chemical properties, but its intracellular functions have not been systematically studied (25, 26). We analyzed the UV-visible spectroscopic properties of Epag by determining the absorption maxima in aqueous buffers at different pH, absorption maxima remained unchanged at 421 nm in the presence and absence of fractionated subcellular suspensions (Supplemental Figure 2, A-B). By assaying the standard dose-dependent increase in absorption (observed up to 80μM; Supplemental Figure 2B) we estimated the fraction of Epag present in the nucleus. We found that nearly 24% of Epag was partitioned into nuclear fraction within 30 minutes of exposure indicating it can diffuse into the nucleus and thus may be accessible to TET2 located in the nucleus (Figure 2A and Supplemental Figure 2C). The purities of the cytoplasmic and nuclear fractions were analyzed by western-blot using specific markers GAPDH (cytoplasmic fraction) and histone H3 (nuclear fraction). The result demonstrated that both fractions used in the study for Epag partitioning are pure and there was no detectable cross-contamination (Figure 2B).

Epag inhibits TET activity independent of TPOR activation. The known functions of Epag have been attributed primarily to its agonistic effect on TPOR. More broad-spectrum effects on hematopoiesis have been postulated to be due to its ability to chelate cellular and extracellular iron (III) (14, 16, 17). To test, if Epag induced TpoR signaling affects TET activity, we engineered murine cell lines BaF3 and 32D to express human TPOR. Irrespective of the presence or absence of TPOR, Epag inhibited TET-dioxygenase activity as indicated by the decrease in 5hmC, a reliable measure of cellular TET-dioxygenase activity (Figure 2, C-E). This effect was irrespective of JAK-STAT pathway activation (mediated by TPO-R activation), as STAT5 phosphorylation levels showed no association with the magnitude of TET-inhibition by Epag (Figure 2, C-E).

Similarly, the presence of TPOR signaling activation did not contribute to TET inhibition by Epag, in human TPOR over-expressing BaF3 and 32D (Figure 2, C-E). While TPO, Epag, and avatrombopag (Apag; a chemically unrelated non-peptidyl TPOR agonist) all activated the JAK-STAT pathway to the same extent in these cells, only Epag exhibited a robust TET-inhibitory effect reflected in the global reduction of 5hmC (Figure 2, C-E). Next, primary murine bone marrow mononuclear cells were treated with vehicle, TPO, Epag, or Apag and we observed that only Epag treatment reduced 5hmC compared to vehicle (Figure 2, F-G). Thus, Epag-mediated TET inhibition in these cells is specific and independent of the presence or absence of TPOR signaling.

Epag treatment phenocopies loss of Tet2. Studies of the consequences of *TET2* mutations in MDS and murine models have demonstrated that loss of *TET2* contributes to HSPCs expansion and myeloproliferation (27-30). Consistent with this, we observed that Epag treatment significantly increased the colony-forming ability of murine HSPCs in vitro (Figure 3A and Supplemental Data 1). Since Epag treatment mimics LOF of *Tet2*, we used $Tet2^{-/-}$ mice as a control to investigate if Epag's effect is indeed *Tet2*-dependent. Consistent with cell-free and suspension cell culture studies, colony-forming assays showed that Epag treatment increased the colony formation in $Tet2^{+/+}$, particularly there were significant increase in CFU-G, CFU-M and CFU-GM while no significant effect was observed in the CFU of $Tet2^{+/-}$ *or* $Tet2^{-/-}$ murine HSPCs (Figure 3B and Supplemental Figure 3A). To recapitulate this effect in vivo, we performed C57BL/6J-CD45.2 $Tet2^{+/+}$ and $Tet2^{-/-}$ syngeneic bone marrow transplant in CD45.1PepBoy mice lethally irradiated with 9.6 Gy radiation followed by Epag treatment (Supplemental Figure 3A). In these single syngeneic bone marrow grafts, Epag treatment significantly increased monocyte and neutrophil counts (Figure 3C and Supplemental Data 1) with no observable change in RBCs, platelets, WBC, or lymphocytes counts of wild type graft recipient mice treated with Epag (Supplemental Figure 3B). Consistent with the results of colony-forming assays the effect of Epag on neutrophils and monocytes was not observed in $Tet2^{-/-}$ graft recipient mice (Figure 3D, Supplemental Figure 3C, Supplemental Data 1). This observation suggested that the effect of Epag observed in murine

hematopoiesis is predominantly due to its inhibitory effects on Tet2. Analysis of the bone marrow from *Tet2*$^{+/+}$ and *Tet2*$^{-/-}$ graft recipient CD45.2 Pep Boy mice after three months of treatment at sacrifice showed that Epag significantly expanded CD34^{+}CD16/32^{+}Lineage^{-}Sca-1^{-}Kit^{+} granulocyte–macrophage progenitor (GMPs) along with a small but significant increase in Lineage^{-}Sca−1^{+}c-Kit^{+} stem cell (LSK) population (Figure 3, E-F, Supplemental Figure 3D and Supplemental Data 1). On the contrary, Epag treatment did not affect the blood or bone marrow composition of *Tet2*$^{-/-}$ graft recipient mice (Figure 3F and Supplemental Figure 3D) compared to the vehicle control group (Figure 3F, Supplemental Figure 3D and Supplemental Data 1).

Epag treatment restricts the clonal evolution of Tet2*$^{-/-}$ *in vivo. Since Epag treatment expands *Tet2*$^{+/+}$ but not *Tet2*$^{-/-}$ cells, we tested if the expansion of wild-type cells can be used to restrict the clonal evolution of *Tet2*$^{-/-}$ cells in vivo using competitive bone marrow transplant in a murine model system. For this purpose, we used lethally irradiated CD45.1 Pep Boy mice as recipients and transplanted them with 2 million chimeric donor bone marrow cells composed of 95% CD45.1 Pep Boy (*Tet2*$^{+/+}$) and 5% CD45.2 C57BL/6J (*Tet2*$^{-/-}$) (Supplemental Figure 3E). Once the graft was established (2 weeks post-transplant) the mice were randomly divided into two groups with one receiving Epag (50 mg/Kg, PO; 5 days/week). The evolution of blood chimerism over time was monitored using the surface markers either using CD45.1, CD45.2, or both (Supplemental Figure 3F). Consistent with the previous reports, *Tet2*$^{-/-}$ cells expanded rapidly in the control group compared to wild-type cells (27-29). Interestingly, Epag treatment significantly slowed the clonal evolution of *Tet2*$^{-/-}$ cells compared to controls (Figure 3G). At the end of the treatment, there was a 26% reduction in the *Tet2*$^{-/-}$ fraction compared to control. Further analysis of different subpopulations of leukocytes demonstrated a bigger difference in monocyte (CD11b^{+}CD11c^{-} Ly6C^{+}Ly6G^{-}) and neutrophils (CD11b^{+}CD11c^{-} Ly6C^{low}Ly6G^{+}) compared to control. After three months of Epag treatment, the *Tet2*$^{-/-}$ fractions of monocytes and neutrophils were nearly half of the control (Figure 3, H-I, Supplemental Figure 3E). We did not observe any change in CD4^{+},

194 $CD8^+$ or $B220^+$ cells in the treatment group compared to controls (Supplemental Figure 3G,
195 Supplemental Data 1).

196 The chimerism of different subpopulations of bone marrow cells at the time of sacrifice was
197 analyzed using CD45.1 and CD45.2 surface marker along with lineage-specific markers for LSKs
198 ($Lin^-Sca\text{-}1^+c\text{-}Kit^+$, stem cell), LKs ($Lin^-Sca\text{-}1^-c\text{-}Kit^+$), GMPs ($CD34^+CD16/32^+Lin^-Sca\text{-}1^-Kit^+$), CMPs
199 ($Lin^-Sca\text{-}1^-c\text{-}Kit^+CD34^+CD16/32^-$) and MEPs ($Lin^-Sca\text{-}1^-c\text{-}Kit^+CD34^-CD16/32^-$)
200 (Supplemental Figure 3H). Epag treatment reduced the rate of clonal evolution of *Tet2*$^{-/-}$ cells in
201 the bone marrow at the time of sacrifice as observed in total *Tet2*$^{-/-}$ cell fraction in the bone marrow.
202 A consistent decrease in LSKs, LKs, GMPs, CMPs, and MEPs fractions was observed, however,
203 the difference did not reach the level of statistical significance (Supplemental Figure 3H,
204 Supplemental Data 1).

205 ***Epag treatment inhibits TET-dioxygenase in primary human hematopoietic cells.*** Epag
206 treatment transiently mimics the loss of TET2 independent of TpoR activation in vitro in murine
207 cells and in vivo transplant models (Figure 3). To test if TET inhibition in human cells is also
208 TPOR-independent, we used primary human bone marrow mononuclear cells derived from
209 healthy donors and treated them with TPO, Epag, Apag, and vehicle alone as a control. Only
210 Epag treatment reduced 5hmC; neither TPO nor Apag had any effect on the global 5hmC, a
211 marker for TET activity in primary bone marrow cells (Figure 4, A-B).

212 The TET inhibitory effect of Epag was further evident by the hypermethylation of the genomic
213 DNA isolated from peripheral blood mononuclear cells (PBMCs) from AA patients (n=16) after
214 Epag treatment. Global 5mC content measured using liquid chromatography with tandem
215 mass spectrometry (LC/MS/MS) demonstrated a significant increase in 5mC content after
216 Epag treatment compared to the PBMCs isolated before treatment (Figure 4C).

217 To further understand the consequences of TET inhibition by Epag in HSPCs, we used a serial
218 re-plating colony-forming assay using human Methocult™. Bone marrow cells from 4 healthy

donors were treated with rTPO or Epag in addition to the standard cocktail of growth factors (SCF, IL-3, IL-6, EPO, G-CSF, and GM-CSF). Epag treatment significantly prolonged the clonogenic potential of healthy bone marrow cells compared to control rTPO treatment as observed in the 2nd and 3rd plating (Figure 4, D-E, and Supplemental Figure 4A). Interestingly, in the 3rd plating, no colony was observed in the control or rTPO treatment, while Epag treated group retained significant colony-forming capacity (Figure 4E). The flow cytometric analysis of cells after the 2nd and 3rd plating showed that a higher proportion of cells (86-97%) in Epag treated cultures expressed CD11b/CD14, compared to control or rTPO groups (Figure 4, F-G, and Supplemental Figure 4, B-E). These results suggest that the effect of Epag may be independent of cMPL status, instead mimicking TET2 loss reflected in increased fractions of $CD11b^+/CD14^+$ cells (31).

Epag treatment prevents the clonal growth TET2^{MT}cells. To further confirm the role of TET2 inhibition in Epag's hematopoietic activity and evaluate its impact on TET2 deficient cells, we performed *TET2* knockdown in $CD34^+$ cells derived from human cord blood using lentiviral TET2 targeting shRNA along with scrambled shRNA (*scr*) control as described earlier (31). Consistent with prior reports (29, 31), knockdown of *TET2* in $CD34^+$ cells resulted in a nearly 3-fold increase in colony numbers compared to *scr* shRNA control. Consistent with the murine model, the Epag treatment of human $CD34^+$, cells transduced with *scr* shRNA increased colonies nearly by 2-folds compared to the vehicle treatment, this increase was not observed in *TET2^{KD}* $CD34^+$ cells (Figure 5A). Interestingly, a consistent decrease in colony number (statistically non-significant) in the TET2 knockdown cells were observed in the Epag treatment group. Recombinant TPO treatment has no significant effect on the colony numbers (Figure 5A).

Recent reports suggest that highly proliferative myeloid leukemia cells are critically dependent on TET3 (32), particularly in the absence of TET2 (23). To test if TET-inhibition by Epag imposes growth restrictions, particularly on TET2 knockout myeloid leukemia cells compared to wild-type cells we tested isogenic THP1*TET2^{KO}* cells generated using CRISPR-Cas9 and treated with

increasing dose of Epag (Figure 5B). *TET2*$^{-/-}$ THP1 cells have a higher sensitivity to Epag compared to the non-targeting gRNA THP1 control cells, suggesting that the inhibition of residual TET activity mostly coming from TET3 may be detrimental for TET2 mutant leukemia cells (32). Thus, while Epag inhibits TET2 in TET-dioxygenase proficient bone marrow cells from AA patients leading to HSPC expansion, in TET2-deficient leukemia cells it may restrict their growth because of their dependence on TET3 for demethylation of promoters and enhancers of survival and proliferative genes. This in-vitro cell line model was further confirmed in primary cells derived from patients with TET2 mutant myeloid neoplasms. The effect of Epag on TET2 mutant myeloid neoplasm patient-derived mononuclear cells were tested in 9 patients (5 with biallelic and 4 with monoallelic inactivation of TET2) using colony-forming assays in the presence or absence of Epag (Figure 5C, Supplemental Figure 5, and Supplemental Table 1). Treatment of Epag led to a nearly 2-fold reduction in the colony numbers compared to vehicle treatment (Figure 5C and Supplemental Figure 5). The effect was more pronounced in the second plating (Figure 5C). We did not observe any statistically significant correlation of Epag treatment with VAF or the Monoallelic or biallelic inactivation under in vitro culture conditions (Supplemental Figure 5, D-E).

Since Epag has been extensively studied in clinical trials and some of the clinical trials have patient mutation data available, we investigated those details and analyzed the publicly available data. In a study with a cohort of 43 AA patients by Winkler et al.,(33) there were 5 patients with TET2 mutations at different points in Epag treatment, among which 3 were LOF truncating mutations and 2 missense alterations of unclear significance (Figure 5D). Interestingly, all 3 truncating TET2 mutants were responders, and these clones completely disappeared at the end of the treatment, suggesting that Epag may have a restrictive effect on otherwise proliferative *TET2*^{MT} clones. In contrast, 2 patients had missense mutations (M865L and L1248P) considered inconsequential for TET2 enzymatic function (Figure 5D). These patients were non-responders, and TET2 mutant clone size did not change in these cases. The results seen within responders with pathogenic mutations agree with our hypothesis that *TET2*^{MT} responding to Epag-mediated

TET-inhibition due to both the proliferative advantage to WT HSPCs, thus competitively restricting and preventing the clonal evolution of *TET2*^{MT} cells as well as preventing the otherwise proliferative dominant clone in certain patients.

Discussion

Newly discovered biologic activities of drugs with seemingly established specificity often lead to new indications, sometimes years after the initial FDA approval. The remarkable efficacy of Epag in AA, a prototypic HSC deficiency disorder, suggests that it may have alternative activity in addition to its known effects on megakaryocytopoiesis. Earlier it was reported that some of its TPOR independent hematopoietic activities are due to intracellular and extracellular iron (III) chelation (14, 16, 17, 21). However, a large part of Epag's mechanisms of action remained unclear. Here, using series of in vitro cell-free and cell-based assays along with in vivo small animal models, we report that parts of Epag's TPOR independent clinical activities may be due to its ability to inhibit TET-dioxygenase by direct interaction with the catalytic domain. This reversible and transient inhibition, to some extent, phenocopies the hematopoietic consequences of TET2 LOF observed in *TET2* mutant cells i.e. expansion of HSPCs and myeloid skewing.

Our results show that while Fe^{2+} is required for Epag binding to TET2, its inhibitory effect is not due to sequestration of intracellular or extracellular iron and cannot be rescued by adding excess iron. Thus, the following two plausible reactions can be envisioned to explain the TET inhibitory activity of Epag:

(i) *TET2* + Fe^{2+} + *Epag* ↔ [Fe^{2+}-*Epag*] + [*TET2*] *or*

(ii) *TET2* + Fe^{2+} + *Epag* ↔ [*TET2*-Fe^{2+}-*Epag*]

The addition of several-fold molar excess α-KG failed to overcome the inhibitory effect of Epag suggesting that it is not a competitive inhibitor of α-KG. Further analysis of direct binding kinetics using SPR, confirmed the specificity of Epag interaction with $TET2^{CD}$ in the presence of Fe^{2+}. Substitution of Fe^{2+} by Fe^{3+} in the binding buffer significantly reduced Epag affinity to $TET2^{CD}$.

Interestingly, 750-fold molar excess Fe^{3+} shifted two-fold IC50 suggesting that Epag chelates Fe^{3+} with the caveat that its affinity for $TET2^{CD}$ is much higher than that for Fe^{3+}. DFO, a known powerful iron chelator, showed no significant binding to TET2 suggesting that Epag's interaction with the TET2 catalytic domain is specific and requires Fe^{2+} as a cofactor. Using a cell-free in vitro model system coupled with in silico molecular docking we demonstrate that Epag directly binds to $TET2^{CD}$ via Fe^{2+} and potently inhibits its dioxygenase function in physiologically relevant doses (34). Therefore, the experimental evidence presented here supports a model where Epag forms a specific tripartite complex [*TET2-Fe^{2+}-Epag*] which traps the catalytic site in an inactive conformation following equation (ii) above.

Epag's effect on TET2 in cell-free systems is clinically as well as biologically relevant since it is partitioned into the nucleus within half an hour to exert its inhibitory activity on TET-dioxygenases in cells as reflected in the reduced genomic 5hmC content. Significant effects of Epag had been observed with 50 mg and 75 mg daily doses in humans (10, 35). Pharmacokinetic characterization of healthy volunteers and patients reported that peak plasma concentration at steady state (Cmax, ss) reaches around 8.0 and 12.7 µg/ml after once-daily oral administration of 50 and 75 mg, respectively (34, 35). Given the Epag molecular weight of 442.5 g/mol, the Cmax is around 10 µM or 20 µM for 50 mg or 75 mg oral dose. In the present study, we observed an IC50 of ~1µM for TET2 inhibition which is more than one-tenth of the physiological concentration achieved for Epag in patients. Consistent with physiological steady-state Cmax, we observed a significant effect of Epag at 10 µM and 20 µM across different cellular assays.

The effect of Epag treatment on DNA dioxygenase activity was independent of TPOR signaling. Epag is known to be human TPOR specific with no known activation of murine JAK-STAT signaling (14, 25, 26), but the effect on TET2 was observed in murine hematopoietic cells in the absence of TpoR activation. Reconstitution of human TPOR in murine cells, restored STAT5 phosphorylation without any measurable changes in the dioxygenase activity. The presence or

absence of the activated JAK-STAT signaling has no bearing on the TET-inhibitory effects of Epag. TPOR independent TET-inhibitory action of Epag was further supported by the fact that another small molecule TPOR agonist (Apag) and recombinant TPO activated STAT5 but have no effect on TET-dioxygenase activity measured in the genomic 5hmC content.

Consistent with its inhibitory effect on TET2 activity, Epag treatment significantly increased the number of CFU in *Tet2*$^{+/+}$ murine HSPCs while this effect was completely absent in *Tet2*$^{-/-}$ bone marrow cells. As expected, lower activity of *Tet2* was associated with a higher baseline expansion rate, and the effect of Epag was not observed in cells with low TET2 activity. This genotype-dependent effect of Epag was even more profound *in vivo*. Epag improved recovery of *Tet2*$^{+/+}$ murine bone marrow recipient in syngeneic transplant in CD45.1 Pep Boy mice with no significant effect observed in mice receiving *Tet2*$^{-/-}$ grafts suggesting that Epag effect can be attributed TET2 inhibition. In a competitive bone marrow reconstitution with a split *Tet2*$^{+/+}$ and *Tet2*$^{-/-}$ graft, Epag provided a proliferative advantage to *Tet2*$^{+/+}$, leading to a significant decrease in *Tet2*$^{-/-}$ fractions of blood cells. Further analysis of different lineages reinforced the notion that Epag treatment mimics loss of *Tet2* as evidenced by myeloid skewing involving monocyte and neutrophil populations and increased numbers of both LSKs and GMPs in *Tet2*$^{+/+}$ fractions with a concomitant decrease *Tet2*$^{-/-}$ fractions of these cells.

Consistent with the TET-inhibitory action of Epag, analysis of the genomic DNA of the PBMCs of AA patients demonstrated a treatment associated increase in the global cytosine methylation, an effect comparable to that observed in normal bone marrow *in vitro* but not with the structurally unrelated TPO-R agonist, Apag or rTPO. This TET2 inhibitory effect of Epag significantly prolonged the clonogenic potential of TET2 proficient bone marrow cells compared to rTPO particularly in the 2nd and 3rd plating with a higher proportion of CD11b^{+}/CD14^{+} cells reinforcing the notion that Epag may be mimicking loss of TET2 in hematopoietic cells (31). We counted all colonies in the dish of human Methocult™ H4435 from STEMCELL Technologies. The Methocult™ H4435 used in our assay was expected to support the growth of erythroid progenitor

cells (BFU-E and CFU-E), granulocyte-macrophage progenitor cells (CFU-GM, CFU-G and CFU-M), and multipotential granulocyte, erythroid, macrophage and megakaryocyte progenitor cells (CFU-GEMM) colony. The addition of Epag also supports the growth of megakaryocytic progenitors (14), which makes it very difficult to differentiate different colony types based on the visual characteristics, so we counted all types of colonies in the different conditions. Furthermore, to objectively determine the impact of experimental conditions i.e., Epag treatment we subjected the harvested colonies for characterization by flow cytometry for the cellular output including granulocytic and monocytic cells. This goes beyond the standard of colony counting with all of its inherent subjectivity including visual assessment. This in vitro observation was consistent with in vivo effect of Epag treatment on C57BL/6J *Tet2* wild-type mice. Serial re-plating experiments demonstrate the self-renewal capacity of stem and progenitor cells. This assay has been used widely to demonstrate the effects of various manipulations of genetic machinery in hematopoiesis, especially for the study of TET2 biology. Previous studies showed that TET2 deletion does not significantly affect CFUs in the first plating but in later serial replating, demonstrating TET2's function in the self-renewal of HSPCs (29, 36). Consistent with these observations, we found that Epag significantly increase CFU in the $2^{nd}/3^{rd}$ plating but not the 1^{st} plating. Several TPO-R agonists demonstrate similar hematopoietic activities in aplastic anemia, including TPO peptide mimetic romiplostim (37, 38), which does not inhibit TET2. In the multilineage recovery of AA patients, the TET-inhibitory effect of Epag may be secondary to TPO-R activation. However, consistent with the durable unique clinical response of Epag in aplastic anemia, TET2 inhibition may be key mechanisms of action that contributes to a prolonged expansion of HSPCs leading to complete response and recovery.

TET dioxygenases are critical regulators of cytosine methylation and thereby a gatekeeper for efficient transcription in mammalian cells (39-41). Here we observed that there is no proliferative advantage of Epag treatment in the absence of TET2, which is very different to its activity in TET2 proficient cells. Recent reports showed that Epag restricts the clonal outgrowth of malignant cells

in general (17, 22, 42-44). Our observations with Epag are consistent with these reports and further indicate that the dioxygenase inhibitory effect of Epag may be contributing to its antineoplastic effect. This is further supported by evidence that TET2 deficient leukemia cells rely on residual TET activity coming from TET1 and TET3 for their proliferative advantage and survival (23, 32). Thus, a further inhibition of TET activity may preferentially restrict the growth of *TET2*^{MT} malignant cells while giving growth advantage to TET2 proficient normal HSPCs (23, 32, 39). However, the effect may be more complicated due to the on-target effect on TPOR that may provide a pro-survival signal by JAK-STAT signaling activation in human cells. Interestingly, analysis of previously reported clinical trial data is in agreement with our hypothesis that TET2-mutant responding to Epag-mediated TET-inhibition in part due to its growth-promoting effects on WT HSPCs and restrictive effect on TET2 mutant cells. Thus, Epag may provide a competitive advantage to normal HSPCs while preventing outgrowth of TET2 mutant malignant cells. Another way to investigate whether Epag restricts the growth of *TET2* mutant cells would be to use mouse models of *TET2*^{MT} CHIP to determine whether the malignant evolution of TET2 CHIP can be restricted or slowed by Epag.

The inhibitory properties of Epag on TET2 as they relate to its efficacy in AA may in part explain the increased risk of clonal evolution to myelodysplastic syndrome, characterized by a high prevalence of monosomy-7 in certain individuals (45). Previously, Epag in combination with 5-Azacytidine (5-Aza) was described to increase the risk of progression in the setting of MDS leading to inferiority when the combination was compared to 5-Aza alone (46). Somatic LOF *TET2*^{MT} are common precursor lesions in MDS and also occur in clonal hematopoiesis of indeterminate potential, an asymptomatic condition credited with increased risk of myeloid neoplasia. It was reported that LOF *Tet2*^{MT} facilitates the acquisition of subsequent mutational hits (47). Interestingly, the clinical trial of Epag in MDS was in combination with 5-Aza, known to upregulate *TET2* and *TET3 (48, 49)* and thus Epag may have counteracted the effect of each other5-Aza. It is possible that the observed increased risk of clonal evolution may be related to

the TET-inhibitory effects of Epag, in TET2 proficient cases phenocopying LOF *TET2*^{MT}. The opposing effects of these two drugs may in part explain the relatively inferior outcome in patients receiving the combination compared to 5-Aza placebo.

In summary, our results indicate that Epag is a clinically relevant DNA dioxygenase inhibitor and this activity may contribute, in addition to its TPOR agonistic effect, to its efficacy in AA including re-expansion of HSPCs. This activity is exclusive to Epag and not observed with thrombopoietin or other TPO-R agonists. As such Epag represents a class of agents with pleiotropic activity as TET dioxygenase inhibitors, conferring broader effects which may prove useful in many applications.

Methods

Key reagents

Reagents used in the study were purchased: Eltrombopag (Epag), MedKoo Biosciences, Cat #100941; Deferoxamine, DFO, SIGMA Cat #D9533; Avatrombopag (Apag), MedChemExpress, Cat #HY-13463; recombinant human TPO (rTPO), PeproTech, Cat #300-18; and recombinant murine TPO (rmTPO), PeproTech, Cat #315-14.

Mice maintenance and experiments

Animal care and procedures were conducted in accordance with Cleveland Clinic institutional guidelines and approved by the Institutional Animal Care and Use Committee (IACUC), Cleveland Clinic. *Tet2* mutant mice (Stock# 023359) were procured from the Jackson lab. In mouse transplant experiments, recipient wild type CD45.1 Pep Boy mice received two doses of 480 rad (4.8 Gy) irradiation delivered 3 hours apart, followed by tail veins injection of 2 million donor bone marrow cells for each mouse. In single transplantation, 100% CD45.2 wild type or $Tet2^{-/-}$ bone marrow cells were used as donor cells. In competitive transplantation, 5% $Tet2^{-/-}$ CD45.2 cells from C57BL/6J mice and 95% $Tet2^{+/+}$ from CD45.1 Pep Boy cells were used as donor cells. Treatment (50 mg/kg Epag freshly dissolved in water, or vehicle p.o. once a day, 5-days/week) started 24 hours post-transplant in single, 2 weeks post-transplant in competitive experiments. Peripheral blood was collected by retro-orbital bleeding for complete blood count by Hemavet 950 (Drew Scientific) and/or flow cytometry analysis by FACSVerse (BD) every month. Mice were sacrificed for bone marrow analysis after three months of treatment. Antibodies used in this study for flow cytometry analysis are presented in Supplemental Table 2.

Tissue culture

Human normal bone marrow (NBM) samples and cord blood cells from healthy donors in accordance with Cleveland Clinic IRB-approved protocols. All patient samples were collected using informed consent. Mononuclear cells were purified by Ficoll (Histopaque®-1077, SIGMA, Cat #10771) from BM and cord blood samples. $CD34^+$ cell purification was performed using CD34

MicroBead Kit (Miltenyi Biotec, Cat #130-097-047). All human primary mononuclear cells including $CD34^+$ cells are maintained in IMDM medium supplied with 20% FBS, 100 U/ml pen-strep, and 100 ng/mL recombinant human SCF (PeproTech, Cat #300-07).

Mouse bone marrow cells after red blood lysis were maintained in IMDM medium supplied with 20% FBS, 100 U/ml pen-strep, and 50 ng/mL recombinant murine SCF (PeproTech, Cat #250-03). 32D and Ba/F3 cell lines were purchased from ATCC (Manassas, VA) and maintained in IMDM culture medium supplied with 10% FBS, 100 U/ml pen-strep, and 2 ng/ml murine IL3 (PeproTech, Cat #213-13).

32D and Ba/F3 were electroporated by Amaxa Nucleofector II with programs E-032 and X-001, respectively, with human TPO-R plasmid MPL-pCMV-3Tag-3a, in which open reading frame of MPL (NM_005373.2) and cloned in pCMV-3Tag-3a vector (GenScript). Stable cell lines were established in culture for 2 weeks in the presence of 500 µg/ml G418 (Gibco, Cat #10131-035).

TET2 mutant cells (T30 and T31), as well as their vector control cells (Vec), were generated and described earlier (23).

Colony-forming assay

Methocult™ M3434 (murine) and H4435 (human) from STEMCELL Technologies were used for colony-forming assays. Methylcellulose was supplied with the indicated concentration of Epag or rTPO before cell seeding. Mouse bone marrow cells after red blood lysis were seeded at the concentration of 30,000 cells per ml. Bone marrow mononuclear cells from healthy donors and patients were seeded at the concentration of 100,000 cells per ml. $CD34^+$ cells were infected with lentiviral TET2 targeting shRNA or non-targeting scrambled shRNA (scr) as described and characterized in our previous study (31). Two days after lentivirus infection, $CD34^+$ cells were seeded at the concentration of 5,000 cells per ml in Methocult™ in the presence of 5 µg/ml puromycin. Colonies were scored and cells were harvested for re-plating or flow cytometry analysis by FACSVerse (BD) on Day 10 to 14.

Expression and Purification of recombinant Catalytic Domains of TET1, 2 and 3

TET2 catalytic domain was purified in the lab. GST-TET2 (1099-1936 Del-insert)(24) expression vector was transformed into Escherichia coli strain BL21(DE3)pLysS. The transformant was grown at 37 °C to an OD600 of 0.6 and switched to 16 °C for two additional hours. Ethanol was added to the final concentration of 3% before induction by adding isopropyl-b-D-thiogalactopyranoside to the final concentration of 0.05 mM. Cells were cultured for 16 hours at 16 °C. Cells from 2 L culture were harvested and lysed in 50 ml of lysis buffer [20 mM Tris-HCl pH7.6, 150 mM NaCl, 1X CelLytic B (Sigma C8740), 0.2 mg/ml lysozyme, 50 U/ml Benzonase, 2mM $MgCl_2$, 1 mM DTT, and 1X protease inhibitor (Thermo Scientific A32965)] for 30 minutes on ice. Lysate was sonicated by an ultrasonic processor (Fisher Scientific FB-505 with ½" probe) with an amplitude of 70% for 18 1-minute cycles (20 seconds on and then 40 seconds off). The lysate was then centrifuged twice at 40,000 g for 20 minutes. The supernatant was filtered through the membrane with a pore size of 0.45 µm. Flowthrough was diluted 4 times with the solution of 20 mM Tris-HCl pH7.6, 150 mM NaCl. GST-TET2 was purified by GE Healthcare AKTA pure by affinity (GSTPrep FF16/10) and gel filtration (Superdex 200 increase 10/300 GL). For gel filtration, buffer of 10 mM phosphate and 140 mM NaCl, pH 7.4, was used. Recombinant TET1 (Epigentek, Cat #E12002-1) and TET3 (BPS Bioscience, Cat #50163) proteins were purchased and used without any further purification.

5hmC ELISA

The 96-well microtiter plate was coated with 10 pmol avidin (SIGMA A8706) in 0.1 M $NaHCO_3$ at a pH of 9.6 in 100 µl followed by biotin-5mC-DNA (IDT) substrate capture at room temperature. $TET2^{CD}$ protein (0.4 µg) in 100 µl assay buffer [50 mM HEPES pH 6.5, 100 mM NaCl, 0.1 mM $Fe(NH4)_2(SO4)_2$ or $FeCl_3$, and varying concentration of AA along with 1 mM 2-OG] were added to each well for 2 hours at 37 °C. Reactions were stopped using 0.05 M NaOH (100 µL) on a shaking platform for 1.5 hours at room temperature. After washing, wells were blocked with 2% BSA in TBST for 30 minutes and incubated with anti-5hmC antibody (Active motif, 39769, 1: 3,000) at 4 °C overnight. After 4X washes wells were incubated with HRP-conjugated anti-rabbit

secondary antibody (Santa Cruz) and developed by adding TMB (SIGMA, T4444). Reactions were stopped by adding 2M H_2SO_4. Optical densities were recorded at 450 nm. TET2 inhibitor screening was performed in 384 well plates.

Surface Plasmon Resonance

Kinetic characterization of TET2 binding to Epag was monitored by surface plasmon resonance (SPR) with a Biacore 3000 (GE Healthcare). Response units (RU), a measure of binding, were monitored as a function of time. To prepare a surface plasmon sensor chip, purified GST tagged $TET2^{CD}$ (purity >90%) was captured by anti-GST antibodies as described previously (31, 50). Varying concentrations of Epag (0-100 µM) in the presence of 25 µM Fe^{2+} or Fe^{3+} and 25 µM 2-oxoglutarate were used as analytes. In all SPR experiments, analyte solutions of different concentrations were passed over the sensor chip containing immobilized protein at a flow rate of 10 µl/min for 5 min, and dissociation was monitored while SPR buffer passed over the chips for an additional 5 min. Data were normalized against a reference channel containing immobilized GST. Surfaces were regenerated using one injection of 1M NaCl in 10 mM NaOH at 40 µl/min for 30 seconds. Analysis, and fitting of data, was performed with BIA-Evaluation software, version 3.2 (Biacore Inc.), with the option for simultaneous Ka/Kd calculations. Sensorgram data was fitted using global fits to yield Ka and Kd simultaneously assuming a 1:1 Langmuir model. Goodness-of-fit was acceptable based on the criterion of $\chi^2 \leq 1\%$ of the observed maximum response (R_{max}).

Computational docking and in silico structural analysis

The crystal structure of TET2 catalytic domain ($TET2^{CD}$) in complex with 5mCpG containing DNA oligo, N-Oxalylglycine (NOG) and Fe^{2+} (protein data bank ID 4NM6) was used to dock 3d optimized Epag. In silico docking experiments of TET2 and AA were performed using Glide in the computational environment Maestro running on a Quantum TXR411-0128R graphical processing unit. Initially, the grid sizes were kept large enough to contain the entire molecule. The most

favored binding poses of AA with TET2 were determined by restricting the NOG/Fe^{2+} binding site. The complex was minimized, and the binding poses were analyzed in UCSF Chimera 1.8.

Spectrophotometric quantification of Epag

For cell suspension, cytoplasmic extract and nucleus suspension preparation, Cells of 32D were treated with indicated concentrations of Epag or left untreated in plain RPMI culture media at density of 1 million/ml for half an hour. Then cells were harvested after treatment and suspended in buffer A (10 mM HEPES, pH 7.8, 10 mM KCl, 1.5 mM MgCl2, 0.34 M sucrose, 10% glycerol) at concentration of 2.5 million/ml (cell suspension). NP40 at final concentrations of 0.2% was added to cells and cells were vortexed for 10 seconds at the highest setting (Vortex genie-2, Scientific Inst). Supernatant was removed to a new tube (cytoplasmic extract) after centrifugation (5 min, 1,300 g, 4 °C). Nuclei pellet was washed twice with buffer A and suspended at same volume of buffer A of cytoplasmic extract (nucleus suspension). To obtain the uv-visible spectroscopic property of Epag, gradient concentrations of Epag were made in different solutions and subcellular fractions prepared from untreated 32D cells. Solutions of 100 µl was added to UV transparent plate (Corning, REF# 3635) and absorbance from 300 nm to 700 nm with 1 nm per step was measured Synergy H1 Hybrid Reader (BioTek).

Protein extraction and western blot

Cell pellets were lysed in RIPA buffer (Thermo, 89900) supplied with 1X protease inhibitor cocktail (Thermo, A32965), 5 mM EDTA and 1X phosphatase inhibitor cocktail 2&3 (SIGMA, P0044 & P5726) on ice for 15 min. Lysate was sonicated by an ultrasonic processor (Fisher Scientific FB-505 with 1/8 inch diameter probe) with setting of 3 for 5 cycles (5 seconds on and then 5 seconds off). After centrifuging (15 min, 20,000 g, 4 °C) supernatant was collected for western blot analyses. STAT5 (Cell Signaling, 94205T), p-STAT5 (Cell Signaling, 9351S), Flag (SIGMA, F1804), β-Actin (Cell Signaling, 4967S), GAPDH (Cell Signaling, 8884S), and Histone H3 (Upstate, 06-755) antibodies were used.

Dot blot

Genomic DNA was extracted using the Purification Kit (Promega, Cat #A1620). DNA samples were denatured in denaturing buffer (0.4 M NaOH/10 mM EDTA) for 10 min at 95 °C and neutralized with equal volumes of 2 M NH4OAc (pH 7.0). The DNA was then spotted on a nitrocellulose membrane using a Bio-Dot Apparatus Assembly (Bio-Rad). The membrane was air-dried, cross-linked by Spectrolinker™ XL-1000 (120 mJ/cm^2), and detected with anti-5hmC (Active motif, 1:5,000) or anti-5mC (Eurogentec, 1:2,500) antibodies. The membrane was stained with methylene blue.

Statistics and Reproducibility

All statistical analyses were performed in GraphPad Prism 8.0 (https://www.graphpad.com/) unless otherwise described. The statistical significance was performed using two tailed student t-test unless described otherwise. To compare multiple experiment one-way ANOVA with Dunnett's test were performed. For each cases a P value less than or equal to 0.05 was considered significant. Each experiment was performed in triplicate at least twice wherever possible.

Study Approval

Animal care and procedures were conducted in accordance with institutional guidelines and approved protocol by the Institutional Animal Care and Use Committee (IACUC) of Cleveland Clinic. Human patient samples used in this study were collected for research purpose using informed consent in accordance with Cleveland Clinic IRB-approved protocol.

Data and material availability

All requests for raw data and specific materials including engineered stable cell lines reported in this manuscript can be made to the corresponding authors. Results of individual repeats are provided as "Supplemental Data 1".

Author Contributions

YG designed research studies, performed experiments, acquired data, analyzed data, and wrote the relevant sections of the manuscript. **MH, DJ, BP, SP, DRG, ADT, and SK** collected data and contributed with reagents. **SS** and **TL** help and perform data analysis. **DL** and **YP** helped with mouse experiments. **MAS, YS,** and **OYM** provided reagents and assisted in writing relevant sections of the manuscript. **JPM** conceived and conceptualization, read and edited the manuscript and generated resources. **BKJ** conceived and conceptualize the idea, designed, supervised the research, acquired and analyzed data, developed the reagents, wrote the original draft edited the manuscript and generated resources for this study.

Acknowledgements

We appreciate the technical assistances from Molecular Biotechnology Core (surface plasmon resonance), Seth Cory lab (32D and Ba/F3 cells), Lily Wang lab (flow cytometry experiments), Laila Terkawi, Ishani Pandit and Cassandra Kerr (patient sample processing) of Lerner Research Institute, Cleveland Clinic. This work was supported in parts by grants from Leukemia and Lymphoma Society (6582-20-LLS to BKJ), Taub Foundation (to JPM and BKJ) and The Edward P Evans foundation Discovery Research grant #EPE2108BJ to BKJ and the NIH (R35HL135795 and RO1 HL132071 to JPM and R01 CA257544-01A1 to BKJ).

Disclosure of Conflicts of Interest

The authors have no conflict of interest.

References

1. Durrani J, and Maciejewski JP. Idiopathic aplastic anemia vs hypocellular myelodysplastic syndrome. *Hematology American Society of Hematology Education Program.* 2019;2019(1):97-104.
2. Ogawa S. Clonal hematopoiesis in acquired aplastic anemia. *Blood.* 2016;128(3):337-47.
3. Dolberg OJ, and Levy Y. Idiopathic aplastic anemia: diagnosis and classification. *Autoimmun Rev.* 2014;13(4-5):569-73.
4. Valdez JM, Scheinberg P, Nunez O, Wu CO, Young NS, and Walsh TJ. Decreased infection-related mortality and improved survival in severe aplastic anemia in the past two decades. *Clin Infect Dis.* 2011;52(6):726-35.
5. Afable MG, II, Tiu RV, and Maciejewski JP. Clonal Evolution in Aplastic Anemia. *Hematology.* 2011;2011(1):90-5.
6. Desmond R, Townsley DM, Dumitriu B, Olnes MJ, Scheinberg P, Bevans M, et al. Eltrombopag restores trilineage hematopoiesis in refractory severe aplastic anemia that can be sustained on discontinuation of drug. *Blood.* 2014;123(12):1818-25.
7. Desmond R, Townsley DM, Dunbar C, and Young NS. Eltrombopag in aplastic anemia. *Seminars in hematology.* 2015;52(1):31-7.
8. Negoro E, Nagata Y, Clemente MJ, Hosono N, Shen W, Nazha A, et al. Origins of myelodysplastic syndromes after aplastic anemia. *Blood.* 2017;130(17):1953-7.
9. Patel BJ, Barot SV, Waldron M, Billings S, Vij A, Sekeres MA, et al. Clonal dynamics of aplastic anemia/paroxysmal nocturnal hemoglobinuria. *Leukemia & lymphoma.* 2020;61(5):1242-5.
10. Bussel JB, Cheng G, Saleh MN, Psaila B, Kovaleva L, Meddeb B, et al. Eltrombopag for the treatment of chronic idiopathic thrombocytopenic purpura. *N Engl J Med.* 2007;357(22):2237-47.

11. Olnes MJ, Scheinberg P, Calvo KR, Desmond R, Tang Y, Dumitriu B, et al. Eltrombopag and improved hematopoiesis in refractory aplastic anemia. *N Engl J Med.* 2012;367(1):11-9.

12. Townsley DM, Scheinberg P, Winkler T, Desmond R, Dumitriu B, Rios O, et al. Eltrombopag Added to Standard Immunosuppression for Aplastic Anemia. *N Engl J Med.* 2017;376(16):1540-50.

13. Bussel J, Kulasekararaj A, Cooper N, Verma A, Steidl U, Semple JW, et al. Mechanisms and therapeutic prospects of thrombopoietin receptor agonists. *Seminars in hematology.* 2019;56(4):262-78.

14. Kao YR, Chen J, Narayanagari SR, Todorova TI, Aivalioti MM, Ferreira M, et al. Thrombopoietin receptor-independent stimulation of hematopoietic stem cells by eltrombopag. *Science translational medicine.* 2018;10(458).

15. Fattizzo B, Cavallaro F, Milesi G, and Barcellini W. Iron mobilization in a real life cohort of aplastic anemia patients treated with eltrombopag. *American journal of hematology.* 2019;94(9):E237-E9.

16. Zhao Z, Sun Q, Sokoll LJ, Streiff M, Cheng Z, Grasmeder S, et al. Eltrombopag mobilizes iron in patients with aplastic anemia. *Blood.* 2018;131(21):2399-402.

17. Vlachodimitropoulou E, Chen YL, Garbowski M, Koonyosying P, Psaila B, Sola-Visner M, et al. Eltrombopag: a powerful chelator of cellular or extracellular iron(III) alone or combined with a second chelator. *Blood.* 2017;130(17):1923-33.

18. Hon GC, Song CX, Du T, Jin F, Selvaraj S, Lee AY, et al. 5mC oxidation by Tet2 modulates enhancer activity and timing of transcriptome reprogramming during differentiation. *Molecular cell.* 2014;56(2):286-97.

19. Kohli RM, and Zhang Y. TET enzymes, TDG and the dynamics of DNA demethylation. *Nature.* 2013;502(7472):472-9.

628 20. Ko M, Huang Y, Jankowska AM, Pape UJ, Tahiliani M, Bandukwala HS, et al. Impaired
629 hydroxylation of 5-methylcytosine in myeloid cancers with mutant TET2. *Nature.*
630 2010;468(7325):839-43.
631 21. Punzo F, Tortora C, Argenziano M, Casale M, Perrotta S, and Rossi F. Iron chelating
632 properties of Eltrombopag: Investigating its role in thalassemia-induced osteoporosis.
633 *PloS one.* 2018;13(12):e0208102.
634 22. Roth M, Will B, Simkin G, Narayanagari S, Barreyro L, Bartholdy B, et al. Eltrombopag
635 inhibits the proliferation of leukemia cells via reduction of intracellular iron and induction
636 of differentiation. *Blood.* 2012;120(2):386-94.
637 23. Guan Y, Tiwari AD, Phillips JG, Hasipek M, Grabowski DR, Pagliuca S, et al. A
638 Therapeutic Strategy for Preferential Targeting of TET2 Mutant and TET-dioxygenase
639 Deficient Cells in Myeloid Neoplasms. *Blood Cancer Discov.* 2021;2(2):146-61.
640 24. Hu L, Li Z, Cheng J, Rao Q, Gong W, Liu M, et al. Crystal structure of TET2-DNA complex:
641 insight into TET-mediated 5mC oxidation. *Cell.* 2013;155(7):1545-55.
642 25. Erickson-Miller CL, Delorme E, Tian SS, Hopson CB, Landis AJ, Valoret EI, et al.
643 Preclinical activity of eltrombopag (SB-497115), an oral, nonpeptide thrombopoietin
644 receptor agonist. *Stem cells.* 2009;27(2):424-30.
645 26. Erickson-Miller CL, DeLorme E, Tian SS, Hopson CB, Stark K, Giampa L, et al. Discovery
646 and characterization of a selective, nonpeptidyl thrombopoietin receptor agonist.
647 *Experimental hematology.* 2005;33(1):85-93.
648 27. Ko M, Bandukwala HS, An J, Lamperti ED, Thompson EC, Hastie R, et al. Ten-Eleven-
649 Translocation 2 (TET2) negatively regulates homeostasis and differentiation of
650 hematopoietic stem cells in mice. *Proceedings of the National Academy of Sciences of*
651 *the United States of America.* 2011;108(35):14566-71.

652 28. Li Z, Cai X, Cai CL, Wang J, Zhang W, Petersen BE, et al. Deletion of Tet2 in mice leads
653 to dysregulated hematopoietic stem cells and subsequent development of myeloid
654 malignancies. *Blood.* 2011;118(17):4509-18.
655 29. Moran-Crusio K, Reavie L, Shih A, Abdel-Wahab O, Ndiaye-Lobry D, Lobry C, et al. Tet2
656 loss leads to increased hematopoietic stem cell self-renewal and myeloid transformation.
657 *Cancer cell.* 2011;20(1):11-24.
658 30. Jankowska AM, Szpurka H, Tiu RV, Makishima H, Afable M, Huh J, et al. Loss of
659 heterozygosity 4q24 and TET2 mutations associated with
660 myelodysplastic/myeloproliferative neoplasms. *Blood.* 2009;113(25):6403-10.
661 31. Guan Y, Greenberg EF, Hasipek M, Chen S, Liu X, Kerr CM, et al. Context dependent
662 effects of ascorbic acid treatment in TET2 mutant myeloid neoplasia. *Commun Biol.*
663 2020;3(1):493.
664 32. Pulikkottil AJ, Bamezai S, Ammer T, Mohr F, Feder K, Vegi NM, et al. TET3 promotes
665 AML growth and epigenetically regulates glucose metabolism and leukemic stem cell
666 associated pathways. *Leukemia.* 2021.
667 33. Winkler T, Fan X, Cooper J, Desmond R, Young DJ, Townsley DM, et al. Treatment
668 optimization and genomic outcomes in refractory severe aplastic anemia treated with
669 eltrombopag. *Blood.* 2019;133(24):2575-85.
670 34. Gibiansky E, Zhang J, Williams D, Wang Z, and Ouellet D. Population pharmacokinetics
671 of eltrombopag in healthy subjects and patients with chronic idiopathic thrombocytopenic
672 purpura. *J Clin Pharmacol.* 2011;51(6):842-56.
673 35. Hayes S, Ouellet D, Zhang J, Wire MB, and Gibiansky E. Population PK/PD modeling of
674 eltrombopag in healthy volunteers and patients with immune thrombocytopenic purpura
675 and optimization of response-guided dosing. *J Clin Pharmacol.* 2011;51(10):1403-17.

36. Cimmino L, Dolgalev I, Wang Y, Yoshimi A, Martin GH, Wang J, et al. Restoration of TET2 Function Blocks Aberrant Self-Renewal and Leukemia Progression. *Cell.* 2017;170(6):1079-95 e20.

37. Lee JW, Lee SE, Jung CW, Park S, Keta H, Park SK, et al. Romiplostim in patients with refractory aplastic anaemia previously treated with immunosuppressive therapy: a dose-finding and long-term treatment phase 2 trial. *Lancet Haematol.* 2019;6(11):e562-e72.

38. Jang JH, Tomiyama Y, Miyazaki K, Nagafuji K, Usuki K, Uoshima N, et al. Efficacy and safety of romiplostim in refractory aplastic anaemia: a Phase II/III, multicentre, open-label study. *British journal of haematology.* 2021;192(1):190-9.

39. Guan Y, Hasipek M, Tiwari AD, Maciejewski JP, and Jha BK. TET-dioxygenase deficiency in oncogenesis and its targeting for tumor-selective therapeutics. *Seminars in hematology.* 2021;58(1):27-34.

40. Scott-Browne JP, Lio CJ, and Rao A. TET proteins in natural and induced differentiation. *Current opinion in genetics & development.* 2017;46:202-8.

41. Wu X, and Zhang Y. TET-mediated active DNA demethylation: mechanism, function and beyond. *Nature reviews Genetics.* 2017;18(9):517-34.

42. Argenziano M, Tortora C, Paola AD, Pota E, Martino MD, Pinto DD, et al. Eltrombopag and its iron chelating properties in pediatric acute myeloid leukemia. *Oncotarget.* 2021;12(14):1377-87.

43. Nevil G, Roth M, Gill J, Zhang W, Teicher B, Erickson SW, et al. Initial in vivo testing of TPO-receptor agonist eltrombopag in osteosarcoma patient-derived xenograft models by the pediatric preclinical testing consortium. *Pediatric hematology and oncology.* 2021;38(1):8-13.

44. Leitch HA, and Vickars LM. Supportive care and chelation therapy in MDS: are we saving lives or just lowering iron? *Hematology American Society of Hematology Education Program.* 2009:664-72.

45. Shallis RM, Ahmad R, and Zeidan AM. Aplastic anemia: Etiology, molecular pathogenesis, and emerging concepts. *European journal of haematology.* 2018;101(6):711-20.

46. Dickinson M, Cherif H, Fenaux P, Mittelman M, Verma A, Portella MSO, et al. Azacitidine with or without eltrombopag for first-line treatment of intermediate- or high-risk MDS with thrombocytopenia. *Blood.* 2018;132(25):2629-38.

47. Pan F, Wingo TS, Zhao Z, Gao R, Makishima H, Qu G, et al. Tet2 loss leads to hypermutagenicity in haematopoietic stem/progenitor cells. *Nature communications.* 2017;8:15102.

48. Manzoni EF, Pennarossa G, deEguileor M, Tettamanti G, Gandolfi F, and Brevini TA. 5-azacytidine affects TET2 and histone transcription and reshapes morphology of human skin fibroblasts. *Scientific reports.* 2016;6:37017.

49. Yan X, Ehnert S, Culmes M, Bachmann A, Seeliger C, Schyschka L, et al. 5-azacytidine improves the osteogenic differentiation potential of aged human adipose-derived mesenchymal stem cells by DNA demethylation. *PloS one.* 2014;9(6):e90846.

50. Jha BK, Polyakova I, Kessler P, Dong B, Dickerman B, Sen GC, et al. Inhibition of RNase L and RNA-dependent protein kinase (PKR) by sunitinib impairs antiviral innate immunity. *The Journal of biological chemistry.* 2011;286(30):26319-26.

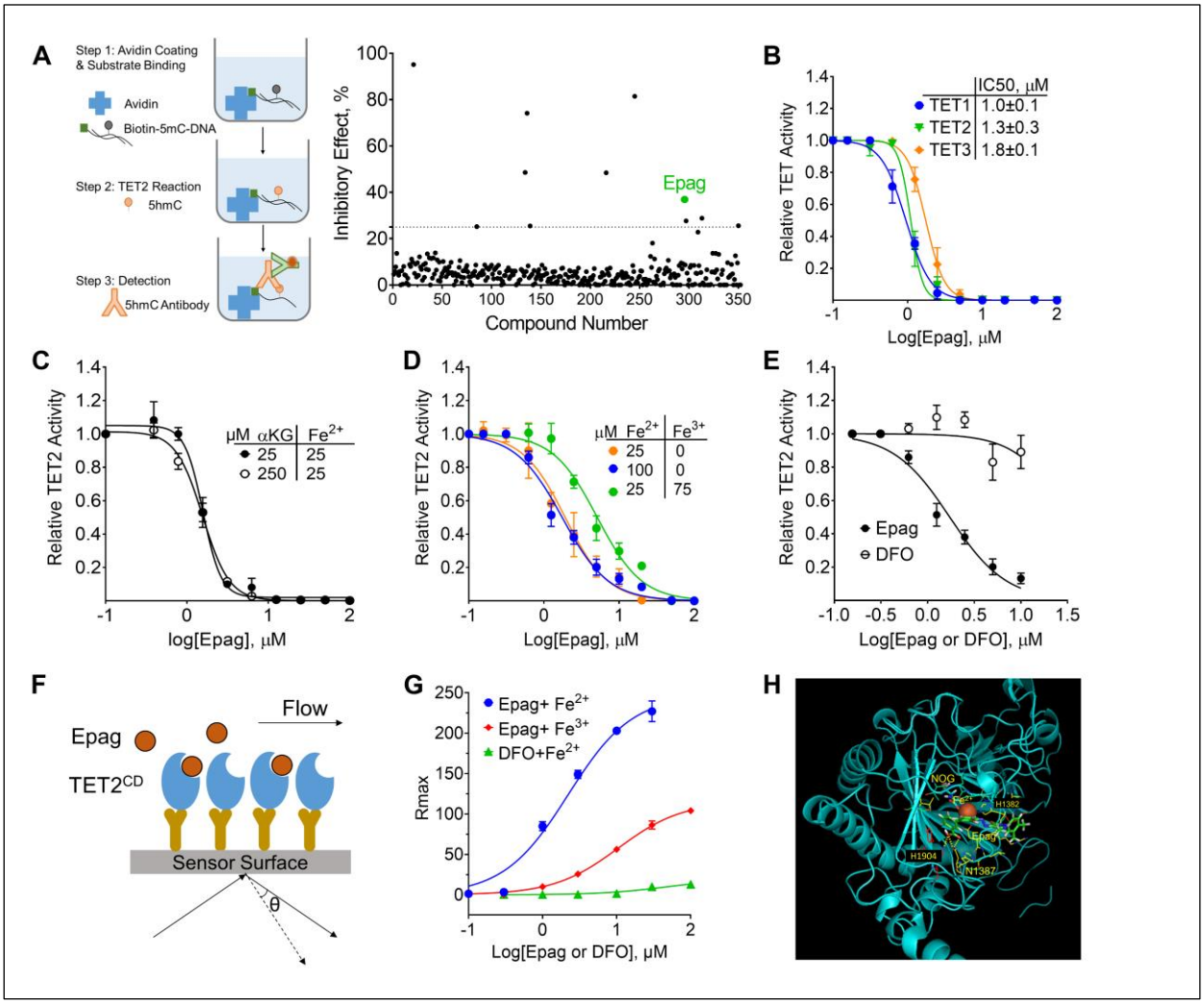

720 **Figure 1. Epag binds and inhibits TET-dioxygenase activity in the presence of iron.** (**A**)
721 Epag as one of the top TET2 inhibitors identified by using an in-house developed ELISA assay.
722 Schematic representation of ELISA assay for TET activity (left). (**B**) IC50 of Epag for TET1, TET2,
723 and TET3 measured by ELISA. (**C**-**D**) TET2 inhibition by Epag cannot be restored by an excess
724 amount of iron (II) or αKG but can only be partially restored by an excess amount of iron (III). (**E**)
725 DFO does not inhibit TET2 activity. TET2 ELISA was performed with different concentrations of
726 DFO and Epag. (**F**) Cartoon of surface plasmon resonance assay to measure the binding affinity
727 of Epag to $TET2^{CD}$. The GST-$TET2^{CD}$ was captured by anti-GST antibody on CM-5 sensor chip
728 along with reference channel GST alone. (**G**) Equilibrium resonance maxima (Rmax) calculated
729 by fitting the kon/koff using 1:1 Langmuir binding by Biaevaluation software and plotted, binding

was measured in the presence of Fe^{2+} or Fe^{3+}. (**H**) Epag mode of interaction with TET2 activated complex. In silico docking simulation of Epag with TET2. (**B**-**E** and **G**) Results are representative of three independent experiments performed and are expressed as mean ± SEM of at least three replicates.

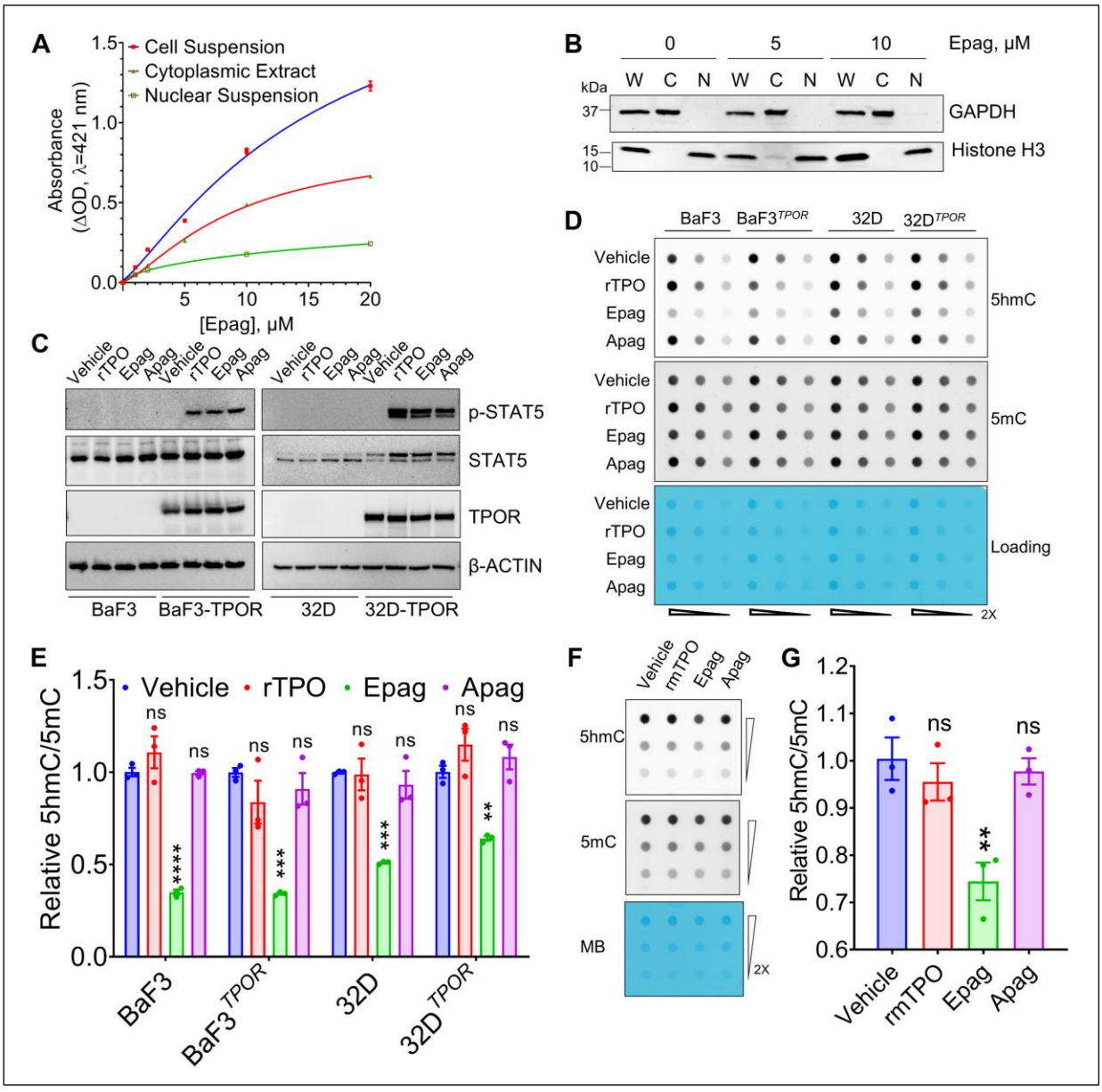

Figure 2. Epag inhibits TET-dioxygenases in cells independent of TPOR. (**A**) Distribution of Epag into different subcellular compartments. 32D cells were treated with Epag for 30 minutes and washed and harvested. Cell suspensions, cytoplasmic extractions, and nuclear pellets were prepared. Absorbance at 421 nm was measured at a known concentration and plotted. The solid

lines are best-fit curves in different fractions. (**B**) Western blot analysis of subcellular fractions of cells treated with Epag. W, whole-cell lysate; C, cytoplasmic fraction; N, nuclear fraction. (**C**) TPO-R activation by rTPO (recombinant human TPO), Epag and Avotrombopag (Apag). Parental or human TPOR overexpressing BaF3, 32D cells were treated with 100 ng/ml rTPO, 1 μM Epag or Apag for 30 minutes. Cells were washed and harvested for protein extraction followed by western blot analysis. (**D** and **E**) after 30 minutes' treatment as described in (**C**), cells were grown for additional 12 hours in complete media prior to genomic DNA extraction for 5hmC and 5mC quantification by dot blot. (**F** and **G**) Epag inhibits TET activity in mouse bone marrow mononuclear cells. Murine BM mononuclear cells were treated with 100 ng/ml recombinant murine TPO (rmTPO), 1 μM Epag or Apag as in panels (**C** and **D**)**,** and 5hmC and 5mC were quantified by dot blot. (**A**-**D** and **F**) Results are representative of three independent experiments performed. (**E** and **G**) data are expressed as mean ± SEM of three replicates. ***P*<0.01, ****P*<0.001, *****P*<0.0001, and ns (*P*>0.05) by one way ANOVA with Dunnett's test of indicated treatment group and the vehicle control.

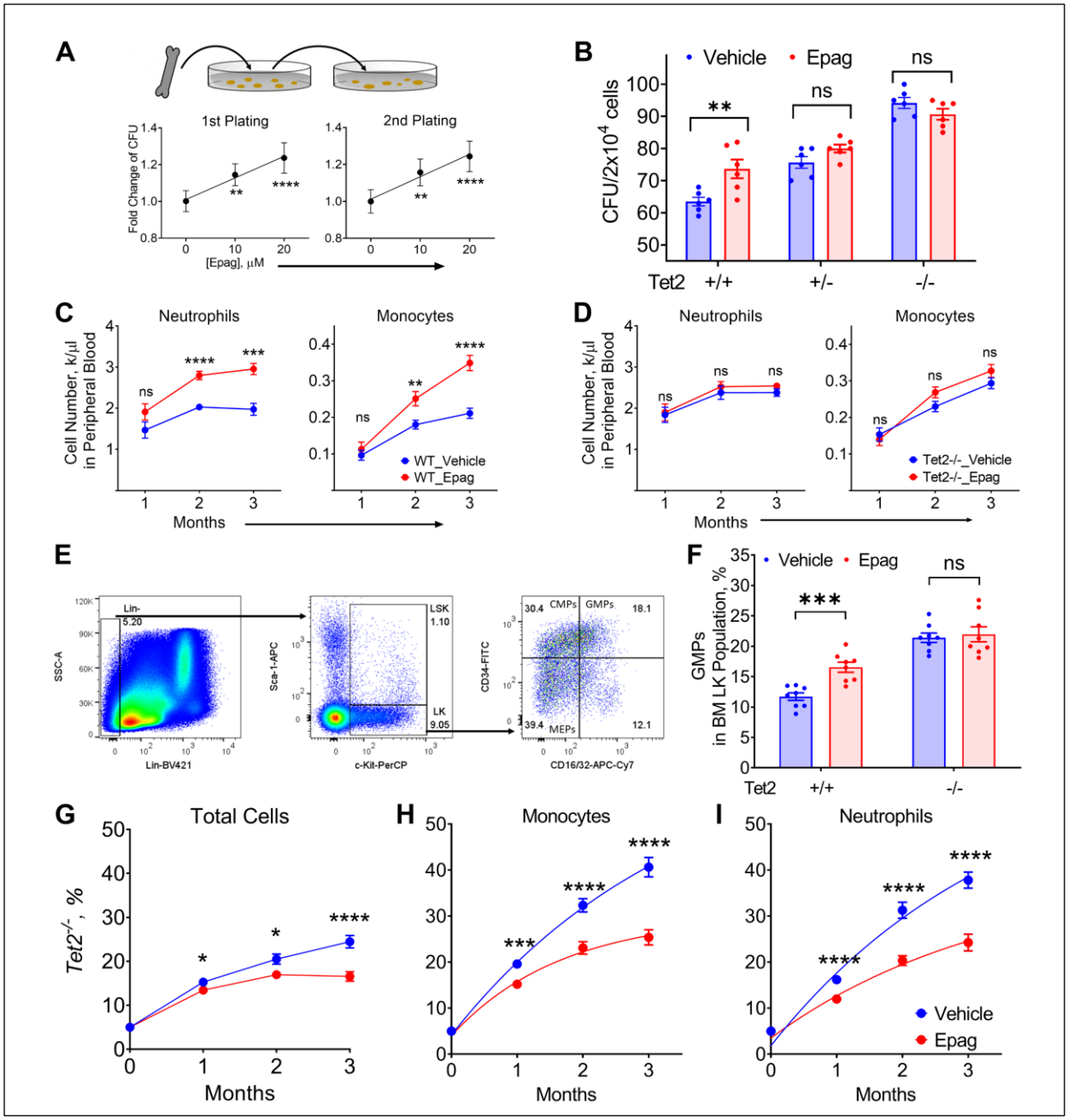

752 **Figure 3. Epag treatment mimics loss of Tet2 and expansion of myeloid compartment is**
753 **Tet2 dependent.** (**A**) Epag dose response in the colony-forming units (CFU) of *Tet2*$^{+/+}$ murine
754 bone marrow cells. (**B**) Epag increased colony-forming units (CFU) in *Tet2*$^{+/+}$ but not *Tet2*$^{+/-}$ and
755 *Tet2*$^{-/-}$ cells. Data of the 2nd plating were shown. (**A** and **B**) six mice per group/treatment were
756 used in 2 independent experiments. (**C** and **D**) Epag significantly increased neutrophil and
757 monocyte count *in vivo* in *Tet2*$^{+/+}$ but not in *Tet2*$^{-/-}$ graft recipient mice. *Tet2*$^{+/+}$ CD45.1, PEP Boy

mice were lethally irradiated prior to the transplant of 2 million *Tet2*$^{+/+}$ or *Tet2*$^{-/-}$ bone marrow cells (CD45.2) via tail vein injection. Peripheral blood samples were counted by HemaVet. (**E**) Gating strategy of flow cytometry analysis for HSPCs, Lin$^-$Sca-1$^+$c-Kit$^+$ (LSK), Lin$^-$Sca-1$^-$c-Kit$^+$CD34$^+$CD16/32$^-$ (CMPs), Lin$^-$Sca-1$^-$c-Kit$^+$CD34$^+$CD16/32$^+$ (GMPs) and Lin$^-$Sca-1$^-$c-Kit$^+$CD34$^-$CD16/32$^-$ (MEPs). (**F**) Epag increased the percentage of GMPs in *Tet2*$^{+/+}$ but not *Tet2*$^{-/-}$ grafted mice. (**G**-**I**) Percentage of *Tet2*$^{-/-}$ cells in indicated populations in bone marrows of transplanted mice. PEP mice were lethally irradiated and received 2 million bone marrow cells consisting of 95% *Tet2*$^{+/+}$ (PEP, CD45.1) and 5% *Tet2*$^{-/-}$ (CD45.2) through tail veil injection. Blood was harvested for flow cytometry analysis, CD11b$^+$CD11c$^-$Ly6C$^+$Ly6G$^-$ (Monocytes) and CD11b$^+$CD11c$^-$Ly6C^{low}Ly6G$^+$ (Neutrophils). The antibodies used are FITC-CD45.1, PE-CD11c, APC-Ly6C, Apc-Cy7-Ly6G, and PerCP-CD11b. Data is representative of experiments done twice. (**C**, **D**, and **F**-**I**) Mice were randomly divided into two groups and either treated with 50 mg/kg Epag or vehicle (water) by oral gavage. A total of 4 donor mice and 8 recipient mice were used per group in 2 independent experiments. Data are expressed as mean ± SEM of eight replicates. **P*<0.05, ***P*<0.01, and ns, *P*>0.05, by one way ANOVA using Dunnett's test (A) and 2-tailed unpaired t test (B-D and F-I).

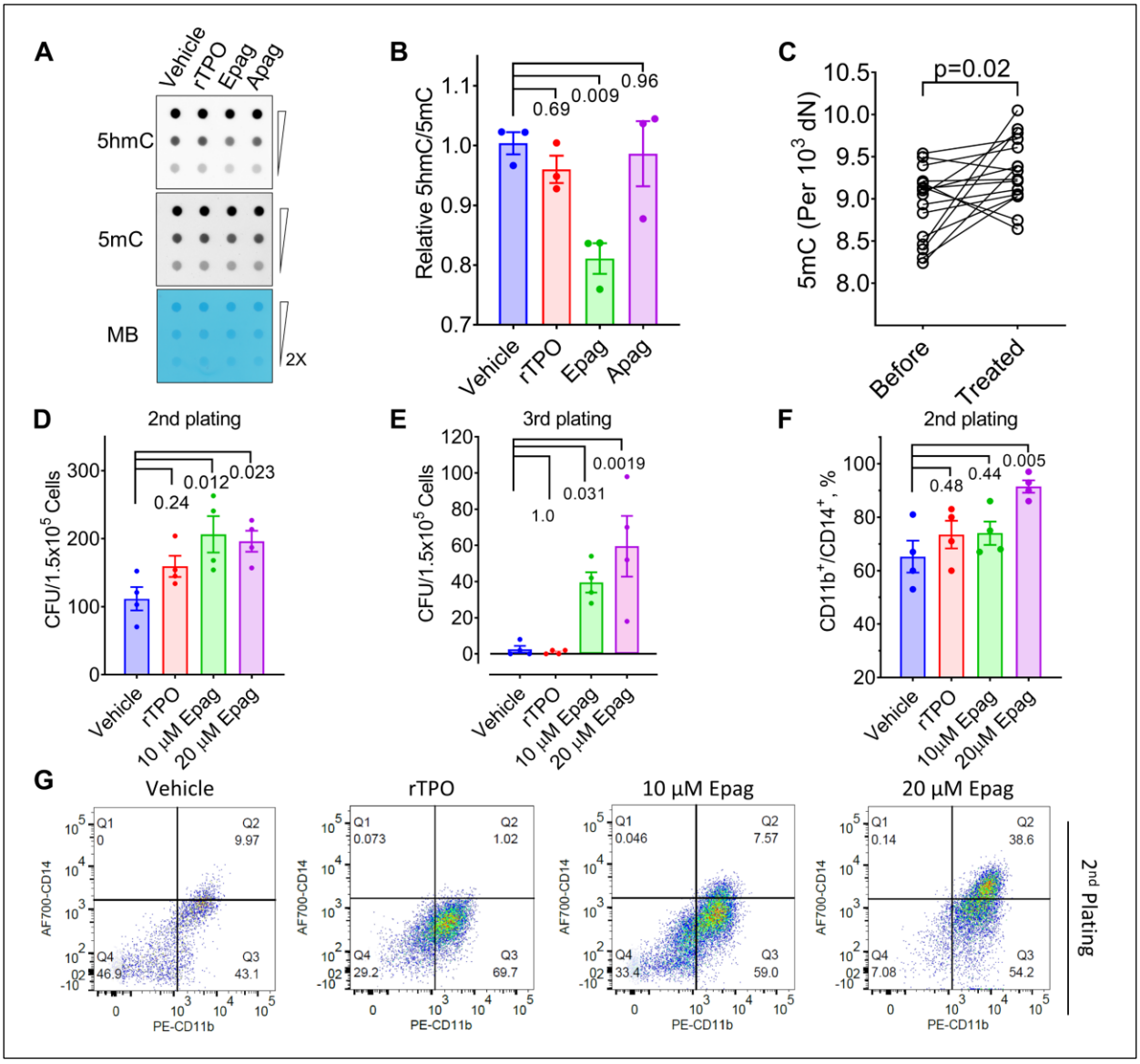

774 **Figure 4. Epag inhibits TET activity in humans.** (**A** and **B**) Epag inhibits TET activity in human
775 bone marrow mononuclear cells. Cells were treated with 100 ng/ml rTPO, 1 μM Epag, or Apag
776 for 30 minutes and followed by culturing for additional 12 hours with 10% FBS and 100 μM
777 ascorbic acid. Cells were washed and harvested for DNA extraction and used for dot blot analysis
778 for 5hmC and 5mC. (**B**) is quantification and analysis of results in (**A**). (**C**) Epag inhibits TET
779 activity in patients. Peripheral blood mononuclear cells from patients with aplastic anemia was
780 isolated before as well as in the middle of taking Epag. Genomic DNA was extracted for mass
781 spectrometer analysis. Taking Epag significantly increased the global 5mC level indicating TET

inhibition by Epag. (**D** and **E**) Epag increases colony-forming units in human bone marrow mononuclear cells from healthy donors (NBMs), n=4. Mononuclear cells were seeded in Methocult™ with indicated concentrations of Epag or 100 ng/ml rTPO. Colony-forming units were counted after the 2nd and 3rd plating. (**F** and **G**) Follow analysis of cells harvested from the 2nd plating of colony-forming assay in (**D**). (**A** and **G**) Results are representative of at least three independent experiments performed. Data are expressed as mean ± SEM of three (**B**) or four (**D-F**) biological replicates in three independent experiments. *P* values from Dunnett's test are indicated.

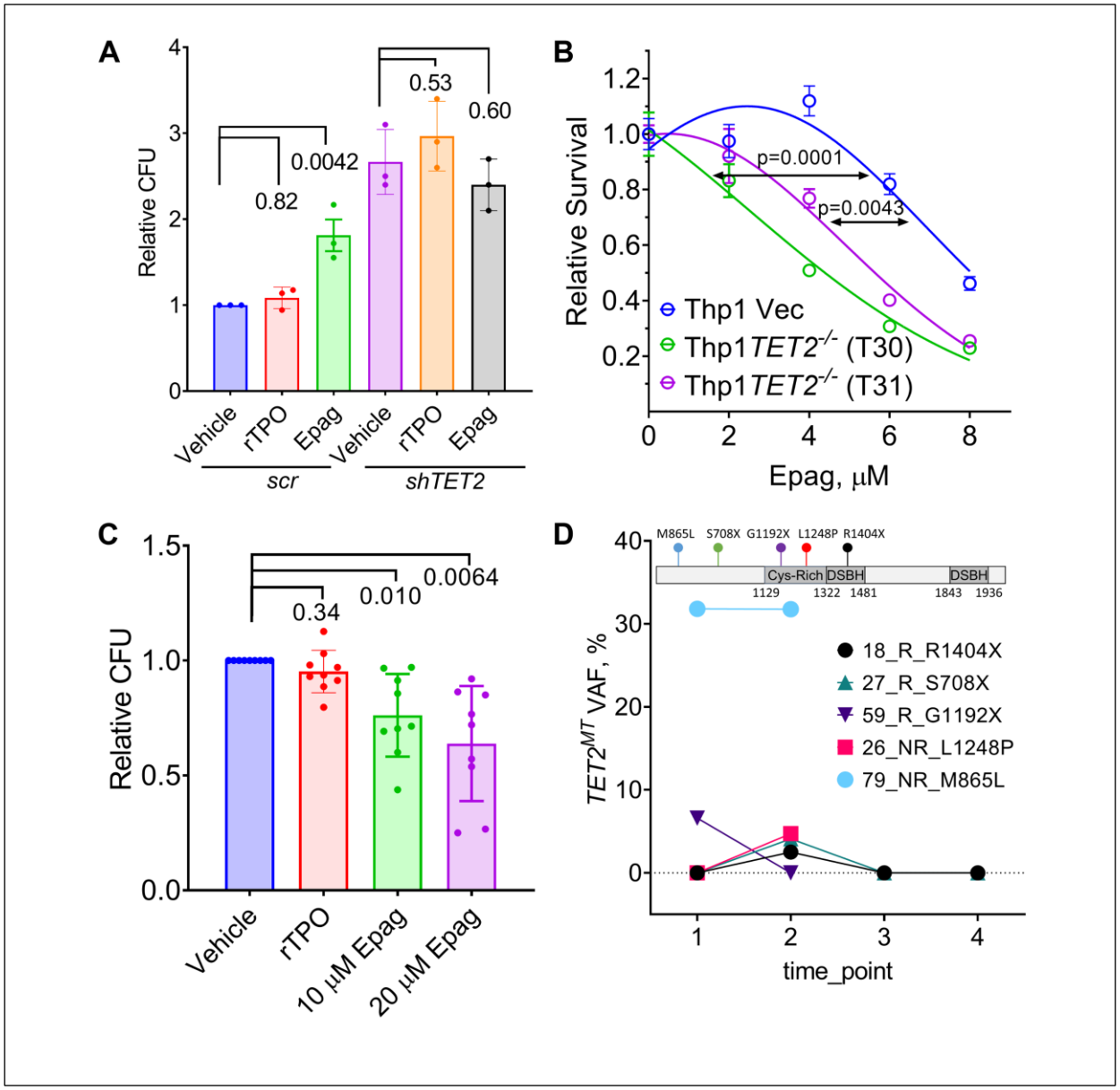

Figure 5. Epag treatment restricts the clonal growth of *TET2^{MT}* malignant cells. (**A**) Epag increased colony-forming units of HSPCs depending on its TET2 inhibitory but not TPOR activation function. CD34+ cells were purified from cord blood samples (n=3) and then infected with lentivirus with TET2 or scrambled shRNA. Cells were plated in Methocult™ 2 days after infection in the presence of puromycin and 10 µM Epag or 100 ng/ml rTPO. Relative colony-forming units presented are after the 3rd plating. (**B**) *TET2$^{-/-}$* cells are more sensitive to Epag treatment. TET2 mutant cells (T30 and T31), as well as vector control cells (Vec), were treated with different concentrations of Epag for 3 days. Cell survival was calculated by CellTiter-Glo

assay. The areas under the curves were calculated and used for statistical analysis. (**C**) Epag significantly restricted the clonal growth of *TET2*^{MT} malignant cells. Mononuclear cells were purified from myeloid neoplasm patient bone marrows (n=9) with TET2 mutations. Mononuclear cells were seeded in Methocult™ with indicated concentrations of Epag or 100 ng/ml rTPO. Colony-forming units were counted after 2nd plating, and relative colony numbers were plotted. (**D**) TET2 mutation variant allele frequency (VAF) of 5 aplastic anemia patients who received Epag treatment, described by Winkler et al., (33). R, responder; NR, nonresponder. Time_points: 1, baseline before Epag initiation; 2, primary end point (24-week); 3, longest time point available on Epag; 4, longest time point available off Epag after achieving robust response. (**B**) Results are representative of three independent experiments performed. Data are expressed as mean ± SEM of three (**A**) or nine (**C**) biological replicates in three independent experiments. *P* values are from one way ANOVA with Dunnett's test are indicated.